

Discussion on the algorithms of a new siphon rain gauge

Hong-yang Li, Qing Li, Xiong Li, Jia-long Song
College of Electric & Mechanical Engineering
China Jiliang University

Higher Education Campus, Zhejiang, Hangzhou, Xue Yuen Street, No. 258
China

freelhy@126.com, lqing55@yahoo.cn, lx_sky@zj139.com, sin0719@163.com
<http://www.cjlu.edu.cn>

Abstract: - As the persistent rain within a short time may trigger off mud-flows and landslides which cause great losses to lives and properties, the real-time monitoring work of rainfall is very meaningful to the disaster early warning. In order to get the accurate rainfall data timely in the unattended wilderness environment, this paper presents a novel siphon rain gauge design based on a strain-type pressure sensor after an integrated consideration of the principles, operation methods, merits and faults of various types of rain gauges. This rain gauge not only keeps the advantages of the traditional siphon rain gauge such as low power and not subject to the restrictions of rainfall's intensity, but also ensures the measurement accuracy by a pressure sensor, besides, the rainfall in the process of siphon can be compensated by the compensation algorithm. Finally, the algorithm optimized data can be transmitted over long-distance through the GSM module on the data collector, thus its scope of application will be greatly increased.

Key-Words: - rain gauge; siphon; low power; long-distance transmission; curve fit;

1 Introduction

Recently the disasters caused by climate anomaly occurred more frequently. Among them, mud flows and landslides which are mainly triggered by the persistent rain within a short time cause great losses to lives and properties.



Fig.1 Landslide in Rio de Janeiro, April 7, 2010

Once such a disaster (as shown in Fig.1) occurred, it is not only causing great losses, but also difficult to carry out the rescue work. Therefore, the real-time monitoring work of rainfall is very meaningful to the disaster early warning. [1]

Rain gauge[2] is the common device used to measure rainfall. Tipping bucket rain gauge[3] (as shown in Fig.2) is now widely used as a remote automatic measurement of rainfall device. When there is 0.1mm's rainfall (depends on the structure), the tip bucket would turn over once, so we can know the rainfall by recording the number of flips. But its accuracy is relatively low, the measurement error is $\pm 4\%$ and if the rain speed is faster, the error will be larger.

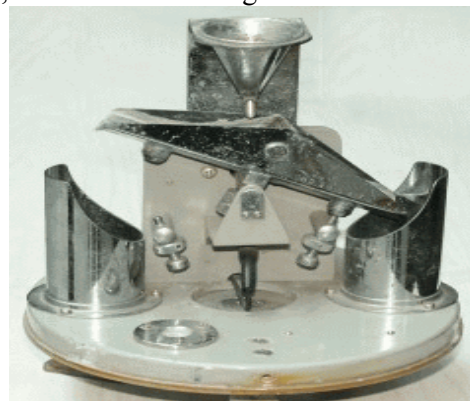


Fig.2 Tipping bucket rain gauge

The measurement error of siphon rain gauge[4] (as shown in Fig.3) is only $\pm 2\%$ and you need not

lines). Then $L_3(t)$ obtained by $L_1(t)$ minus $L_2(t)$ is the rainfall line in once siphon process, the height of $L_3(t)$ means Δh_N .

$h(t)$ represents the actual water level changes in the measuring chamber during the rain (As shown in Fig.5), so the rainfall expression with compensation in once siphon cycle (O → A → B) is:

$$h_s(t) = \begin{cases} h(t); 0 \leq t \leq t_1 \\ h_N + L_3(t) = h_N + L_1(t) - L_2(t); t_1 \leq t \leq t_2 \end{cases} \quad (1)$$

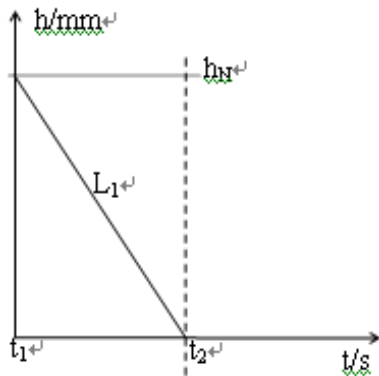


Fig.6.1 Siphon process with rain L_1

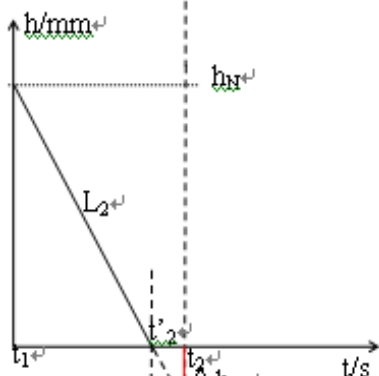


Fig.6.2 Siphon process without rain L_2

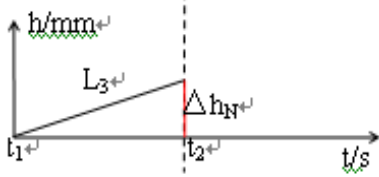


Fig.6.3 Rainfall during the siphon process L_3

Fig.6 The analysis diagram of omission rainfall Δh_N in once siphon drainage

$h(t)$ is measured by the measuring system shown in Fig.4. And t_2 is proportional to the rain rate, if the rainfall rate is faster, then the t_2 is longer. Thus, the time of each single siphon cycle is unequal usually. The value of h_N is determined by the location of

siphon tube, which is a constant value after the structure of measuring system fixed.

According to the formula (1), the rainfall at any time can be expressed as:

$$h_{rain}(t) = K \cdot \left[n \cdot h_N + \sum_{i=0}^n \Delta h_N(i) + h_{s(n+1)}(t) \right] \quad (2)$$

$\Delta h_N(i)$ is the rainfall between t_2 and t_1 when the siphon phenomenon occurring $i+1$ times, which is shown in Fig.6.3. n , means the siphon process happened n times. K , is a scale coefficient making the water level in the measuring chamber converted into the rainfall. $h_{s(n+1)}(t)$ represents the $n+1$ times' $h_s(t)$, according to the formula (1), $h_{s(n+1)}(t)$ is expressed as:

$$h_{s(n+1)}(t) = \begin{cases} h(t); t_{2n} \leq t \leq t_{(n+1)} \\ h_N + L_3(t) = h_N + L_1(t) - L_2(t); t_{(n+1)} \leq t \leq t_{2(n+1)} \end{cases} \quad (3)$$

Formula (3) expresses the rainfall at any cycle of the water level in the measuring chamber rising by rainfall and declining by siphon drainage. When $n=0$, it indicates the first cycle. $t_{2(n+1)}$ is determined by the moment of the lowest point shown in Fig.6.1, what can be realized by the appropriate procedures in the MCU used in the measurement system. After getting the $t_{2(n+1)}$, then extending $L_2(t)$ to $t_{2(n+1)}$ and obtaining $L_2(t)$'s value through the appropriate procedures in the MCU. As $L_1(t)$'s value is known during $t_{1(n+1)} \leq t \leq t_{2(n+1)}$, we can obtain $h_{s(n+1)}(t)$ by formula (3). Substituting the $h_{s(n+1)}(t)$ to formula (2), we derive the rainfall value $h_{rain}(t)$.

3 Linear Fitting

According to the analysis of Fig.6, we first get the experimental curve of $L_2(t)$ that is the siphon process with no rain (As shown in Fig.7). It should be clear that there is no more water added into the measuring chamber during the entire process of Fig.7. However, as the water inside the measuring chamber is surging at the beginning of siphon, resulting in the changes in water pressure, so the measurements of pressure sensor will appear on waving. Thus, the actual height of water level causing the siphon phenomenon should be h_N (As shown in Fig.7). And for the same reason, similar phenomenon also occurs at the end of siphon process (h_0 , the end height of the siphon process with no rain), so the duration of $L_2(t)$ is $t'_2 - t_1$. Then, we get the $L_2(t)$ by intercepting the data between t_1 and t'_2 .

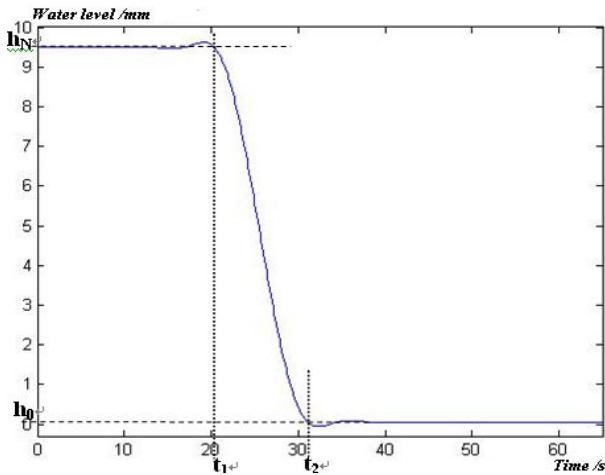


Fig.7 The siphon process with no rain

For the actual data of siphon process expresses as a curve rather than a straight line, while the theoretical analysis of Fig.6 is based on the siphon process expressed as a straight line. Therefore, we first try to find an appropriate straight-line fitting algorithm to handle the $L_2(t)$ in order to make it be consistent with the theoretical analysis.¹

The relatively simple algorithms of linear fitting include:

Algorithm(A): The straight-line passes the starting point and the end point of the original curve;

Algorithm (B) : Using the least squares method on the original curve;

In addition, taking that $L_2(t)$ only bend in the initial as well as the end of the segment while the majority of the middle of the process of maintaining good straight-line condition into account (As shown in Fig.8), we suppose that the slope of the middle segment is the slope of the whole siphon process.

Thus, the algorithm (C) : Using the least squares method on the middle segment of original curve, then fitting the original curve with the slope.

¹ Note: the actual data of $L_1(t)$ also expresses as a curve, so the algorithm also applies to $L_1(t)$

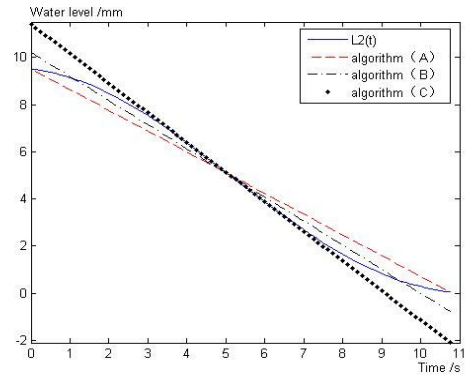


Fig.8 The results of three straight-line fitting algorithm

Using the algorithm (A), (B), (C) on the $L_2(t)$ respectively, the results of fitting are shown in Fig.8. The sketch map of linear fitting is shown in Fig.9. The major advantage of linear fitting method is relatively easy and simple, but as it need to do algorithm on the data of $L_1(t)$ at the same time, so it makes destruction on the original data.

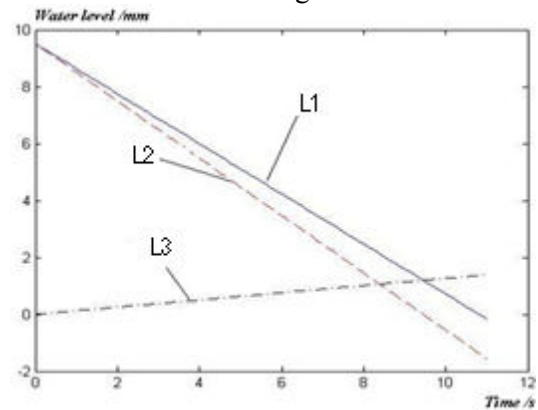


Fig.9 The sketch map of linear fitting

4 Curve Fitting

For the straight-line fitting algorithm, it is need to fit the $L_1(t)$ and $L_2(t)$ both. Moreover, there is an another idea of the algorithm, that is, keeping the $L_1(t)$ unchanged, only using algorithm to $L_2(t)$. In addition, considering the shape of actual siphon process is like an "inverted-S"[5] instead of a straight line, therefore, if the shape of the algorithm result could also be an "inverted-S", that should be more like the real situation, and may improve the accuracy of rain gauge consequently.

The theory of new algorithm is as follows: Based on the actual experimental conditions, the MCU get the total number of 87 sampling points. Combining the idea of algorithm (C), we take the middle segment as the boundary, and then divide the $L_2(t)$ into three sections (As shown in Fig.10).

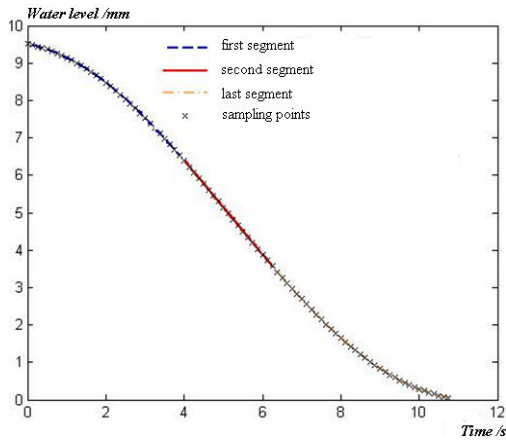


Fig.10 The map of piecewise fitting

The first segment's sampling points with a total number of 32, are from number 0 to 31; the second segment's sampling points with a total number of 19, are from number 32 to 50; and the last segment's sampling points with a total number of 36, are from number 51 to 86. Then, using the least-squares method to fit each segment of data respectively, the result is:

$$f_1(t) = 0.0079 \times t^3 - 0.1800 \times t^2 - 0.1894 \times t + 9.5026; \tag{4}$$

$$f_2(t) = -1.2546 \times t + 11.4142; \tag{5}$$

$$f_3(t) = 0.0070 \times t^3 - 0.0580 \times t^2 - 1.3421 \times t + 12.5302; \tag{6}$$

Through many experiments, we find that the shapes of $L_1(t)$ at the various rate of rain are similar to the $L_2(t)$ that is an "inverted-S". In order to ensure the shape of $L_2(t)$ after the process of algorithm still be an "inverted-S", we could just extend the middle segment of $L_2(t)$ until the same length as $L_1(t)$ without changing the other two segments' shape. We name the curve fitting algorithm (D).

The concrete realization of algorithm (D) is as follows:

When there is rain and cause the siphon phenomenon, we first get the data of $L_1(t)$ and also the number of sampling points N_x . We could also know the duration t_x of $L_1(t)$ based on the sampling frequency set by the MCU. The first 32 sampling

points' data of $L_2(t)$ ($N \in [0, 31]$) could be derived by the formula (4). Next, we intend to get the last 36

sampling points' data of $L_2(t)$ ($N \in [N_x - 35, N_x]$).

After converting N into t based on the sampling frequency, we could get the last segment of $L_2(t)$ by

substituting t into the formula (6). The remaining points are belong to the middle segment of $L_2(t)$ ($N \in [32, N_x - 38]$). In the same way, we could get the middle segment of $L_2(t)$ by substituting t into the formula (5). Finally put the three segments together and it will be $L_2(t)$. Similarly, $L_1(t)$ minus $L_2(t)$ is the result of rainfall calculated by the algorithm (D). The sketch map of curve fitting is shown in Fig.11. The major advantage of curve fitting method is maintaining the original data of $L_1(t)$ better.

5 Inverse method

After doing a lot of experiments at different rain speed, we found that the siphon processes are not the same.

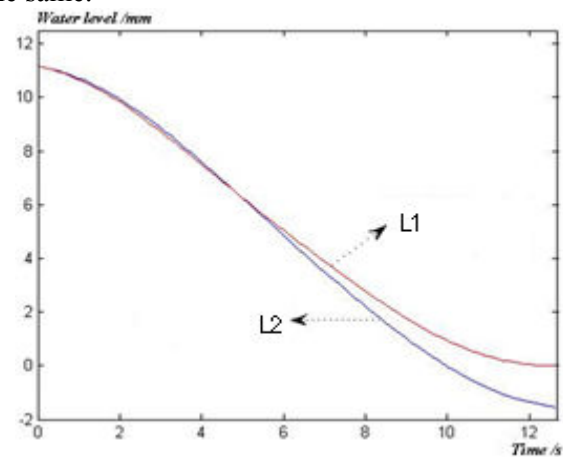


Fig.11 The sketch map of curve fitting

The first section of siphon processes at different rain speed is shown in Fig.12. So, in order to make the algorithm more precise, we should take the speed of rain into account.

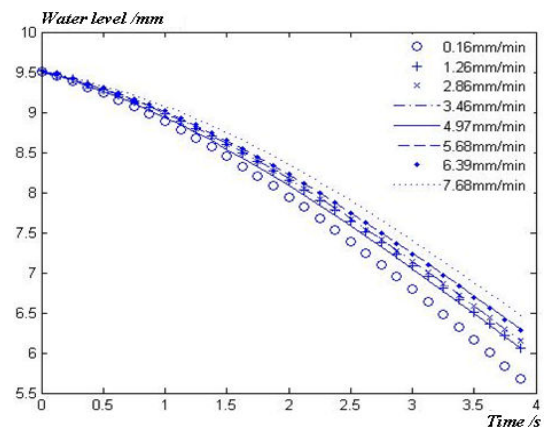


Fig.12 The first section of siphon process at different rain speed

On the premise of having enough experimental data at the various speed of rain, we can also consider using the algorithm (E): inverse method.

The idea of algorithm (E) is as follows:

In the experiments, the rate of simulated rain is controlled by the tap, so the rate is almost constant in once siphon cycle (O→A→B, as shown in Fig.2).

We could know the actual rainfall during the siphon process according to the rate of simulated rain (the slope of O-A segment) and the duration of $L_1(t)$. We take the actual rainfall during the siphon process as $L_3(t)$, and then the result of $L_1(t)$ minus $L_3(t)$ should be the ideal $L_2(t)$, here being recorded as $L_2'(t)$. If you have got enough experimental data of $L_2'(t)$ at a certain rate section already, then you will be able to fit these data by least-squares method to get the expression of $L_2(t)$ under the certain rate section.

In the 0.01mm/min ~ 8mm/min rain rate, we divide it into eight sections with 1mm/min interval, then deduce the expression of $L_2(t)$ under the eight rate section respectively, as shown in Fig.13:

$$L_2(t)_1 = -0.00043254 \times t^4 + 0.021926 \times t^3 - 0.2434 \times t^2 - 0.26995 \times t + 9.4763;$$

$$L_2(t)_2 = -0.00038937 \times t^4 + 0.019655 \times t^3 - 0.2180 \times t^2 - 0.39501 \times t + 9.4899;$$

$$L_2(t)_3 = -0.00022162 \times t^4 + 0.0152 \times t^3 - 0.18184 \times t^2 - 0.55043 \times t + 9.5149;$$

$$L_2(t)_4 = -0.00014334 \times t^4 + 0.013493 \times t^3 - 0.1739 \times t^2 - 0.47793 \times t + 9.5247;$$

$$L_2(t)_5 = -0.0001613 \times t^4 + 0.012822 \times t^3 - 0.15672 \times t^2 - 0.54779 \times t + 9.5349;$$

$$L_2(t)_6 = -0.0001046 \times t^4 + 0.011058 \times t^3 - 0.14936 \times t^2 - 0.49329 \times t + 9.5458;$$

$$L_2(t)_7 = -0.0001541 \times t^4 + 0.012003 \times t^3 - 0.15119 \times t^2 - 0.53565 \times t + 9.5476;$$

$$L_2(t)_8 = -0.0001482 \times t^4 + 0.011978 \times t^3 - 0.16478 \times t^2 - 0.42741 \times t + 9.5419;$$

Fig.13 The $L_2(t)$ expression under various rain rate

6 Comparison of algorithms

As there are many factors in practice will affect the actual results of these algorithms, such as: the actual height of siphon h_N , the sampling frequency set by the MCU, the scale coefficient K , etc. In a word, we can not judge the performance of the algorithm only on a set of experimental samples, but should be concrete analysis of concrete conditions.

From Table.1 to Table.4, they show the four error analyses by using four different algorithms under four different conditions.

For the perspective of error, the algorithm (E) is the best; however, it is required to consider the rain rate, so the design of system and program would be more complex. In contrast, the error of algorithm (B) and (C) is not as good as algorithm (E), but it can also

meet the design requirements. In addition, the theory of linear fitting is easier, so the design of system and program would be easier.

In practice, according to the difficulty of the algorithm, will general first consider the linear fitting algorithm, followed by the curve fitting algorithm, then to consider the inverse method, until find the appropriate algorithm to meet the measurement requirements.

7 Performance of system

Through the comparison of the performance between the new rain gauge and the other representative rain gauges currently on the market, proving that the new siphon rain gauge have certain advantages in the resolution, indication error, measurement error and the rainfall measuring range all, as shown in Table.5.

Table.5 The comparison between rain gauges

Rain gauge model	Resolution /mm	Indication error /mm	Measurement error	Rainfall measuring range
JSP-01 Tipping bucket	0.1	±0.1	±2%	0.01 ~ 6
SJ-1 siphon	0.05	±0.05	±2%	0.05 ~ 4
New siphon	0.01	±0.01	±1%	0.02 ~ 50

8 Outlook and Conclusion

The new siphon rain gauge with certain compensation algorithm can realize the remote data transmission and low power consumption. Besides it has high resolution that can reach 0.01mm. Furthermore, its' rainfall measuring range is so wide that it is not limited by the rain speed. At last, the measurement error of rain gauge is within ±1%.

Although the rain gauge has such good performance, it still hasn't reached the level of application yet. The main reason is that the drift characteristic of the pressure sensor is unsatisfactory which is shown in Table.6.

Through anglicizing the data of Table.6, we can draw the following conclusions:

1. The temperature characteristics of the pressure sensor is non-linear;
2. In a certain temperature, the output of the pressure sensor is not very stable, the fluctuation

range is about 0.02 mV which converted into rainfall is 0.14mm drift. Therefore, the output of the pressure sensor must be filtered, making it more stable, in order to meet the measurement design;

3. When the temperature increased 5 °C, the output of the pressure sensor changes in different increments, the range between the -0.101 mV ~ 0.01 mV, reflecting on the rainfall is -0.7mm ~ 0.07mm. However, the error caused by the drift of temperature can't be filtered, it need a proper compensation circuit for temperature drift. So the next step is to focus on the development of compensation circuit for temperature drift

9 Acknowledgements

This research has been supported by the major science and technology project of Zhejiang Province, with a grant number 2006C13024, and also by the Electric & Mechanical Engineering College of China Jiliang University. The authors appreciate and recognize the funding support from these institutions.

References:

- [1] *The technical requirements and test methods of automatic rain gauge device*. China National Environmental Protection Bureau. 2005.
- [2] *The technical requirements of rain gauge*. China National Machinery Industry Bureau. 1999.
- [3] *Tipping bucket rain gauge*. China National Quality Supervision, Inspection and Quarantine Bureau. 2002.
- [4] *The technical requirements of siphon rain gauge*. China National Machinery Industry Bureau. 1999.
- [5] Wu Hehai, Study of Mathematic Model for Fitting S Shape Distributed Data. *Geomatics and Information Science of Wuhan University*, Vol. 34 No. 4,2009, pp.474-478.
- [6] NAZARIO D. RAMIREZ-BELTRAN1, ROBERT J. KULIGOWSKI2, JOAN M. CASTRO3, A Satellite Rainfall Detection Algorithm. *Proceedings of the 8th WSEAS International Conference on Instrumentation, Measurement, Circuits and Systems*, pp.61-66.
- [7] Ding Kehui, Xi Pingyuan, Liu Shuchun, The Parameter Curve Optimal Approximating Based on MATLAB. *MACH INE TOOL & HYDRAUL ICS*, Vol. 37 No. 3,2009, pp.162-164.
- [8] Bao Jian, Zhao Jianyong, Zhou Huaying, Study on method of curve simulation based on BP network. *Computer Engineering and Design*, Vol.26 No. 7,2005, pp.1840-1842.
- [9] Tong Renyuan, Li Qing, Relationship between Impedance and Elongation of Double-Layers Solenoid. *Proceedings of the 8th WSEAS International Conference on Instrumentation, Measurement, Circuits and Systems*, pp.176-182.
- [10] Gao Wei, Jiang Shuisheng, Method of deal with data error by subsection curve fitting and discrete degree. *CHINA MEASUREMENT TECHNOLOGY*, Vol. 31 No. 6,2005, pp.55-56.
- [11] Hen-Chia Hsu, Jia Hau Chen, Kuang-Yao Lin, A Design of a Type of Heat Measurement Instrumentation. *Proceedings of the 8th WSEAS International Conference on Instrumentation, Measurement, Circuits and Systems*, pp.49-54.
- [12] Chen Shihai, Mao Huiqiong, Niu Guangdong, Design on the Digital Rain- gage with Ultra-low Power Consumption. *SCI-TECH INFORMATION DEVELOPMENT & ECONOMY*, Vol.16 No. 16,2006, pp.181-182.
- [13] Shi Ge, Li Qing, A New Soil Water Content Sensor with Temperature Compensation Design. *Proceedings of the 8th WSEAS International Conference on Instrumentation, Measurement, Circuits and Systems*, pp.263-270.
- [14] Yanjie Wang, Qing Li, Xiong Li, Specific Cylindrical Metal's Distinction in Particular Evironment. *Proceedings of the 8th WSEAS International Conference on Instrumentation, Measurement, Circuits and Systems*, pp.194-199.

Appendix 1

Table.1 Error analysis of algorithm B

Rain rate (mm/min)	0.024	0.255	1.046	2.483	4.688	6.142	6.311	8.134	9.321	14.22
										5
Real rainfall (mm)	11.44	11.56	11.67	11.99	12.41	12.71	12.77	13.19	13.61	14.76
	8	3	5	3	6	8	5	8	2	4
Absolute error (mm)	0.060	-0.00	0.037	-0.09	-0.19	-0.21	-0.09	-0.12	0.079	-0.24
		5		9	9	5	1	5		0
Absolute error without algorithm (mm)	0.005	0.054	0.223	0.534	1.028	1.372	1.436	1.902	2.316	3.653
Measuremen t error (%)	0.52	-0.05	0.32	-0.83	-1.60	-1.69	-0.71	-0.94	0.58	-1.62

Table.2 Error analysis of algorithm C

Rain rate (mm/min)	0.143	0.341	1.111	2.757	4.776	6.082	6.575	7.639	9.221	13.91
										2
Real rainfall (mm)	11.25	11.28	11.43	11.78	12.18	12.46	12.62	12.80	13.25	14.47
	7	8	9	3	5	5	8	2	4	3
Absolute error (mm)	0.004	0.097	0.045	0.004	-0.16	0.093	0.034	0.028	0.112	-0.07
					2					3
Absolute error without algorithm (mm)	0.028	0.066	0.217	0.546	0.956	1.243	1.399	1.665	2.086	3.308
Measurem ent error (%)	0.03	0.86	0.39	0.03	-1.33	0.75	0.27	0.22	0.84	-0.51

Table.3 Error analysis of algorithm D

Rain rate (mm/min)	6.895	10.939	12.413
Real rainfall (mm)	12.629	13.578	13.959
Absolute error (mm)	0.049	-0.058	-0.092

Absolute error without algorithm (mm)	1.454	2.421	2.799
Measurement error (%)	0.386	-0.43	-0.66

Table.4 Error analysis of algorithm E

Rain rate (mm/min)	0.16	1.26	2.86	3.27	4.95	5.64	6.38	7.65
Real rainfall (mm)	9.544	9.754	10.033	10.145	10.461	10.617	10.790	11.060
Absolute error (mm)	-0.031	0.080	-0.003	-0.049	-0.005	-0.022	0.007	0.070
Absolute error without algorithm (mm)	0.034	0.237	0.542	0.627	0.950	1.119	1.265	1.549
Measurement error (%)	-0.32	0.82	-0.03	-0.48	-0.04	-0.20	0.06	0.63

Table.6 The drift characteristic of the pressure sensor

Temp/□	Minimum output/mV	Maximum output/mV	Fluctuation/mV	The increment of minimum/mV	The increment of maximum/mV
0	2.056	2.084	0.028		
5	1.981	1.998	0.017	-0.075	-0.086
10	1.877	1.898	0.021	-0.104	-0.1
15	1.804	1.823	0.019	-0.073	-0.075
20	1.736	1.757	0.021	-0.068	-0.066
25	1.653	1.671	0.018	-0.083	-0.086
30	1.663	1.681	0.018	0.01	0.01
35	1.632	1.655	0.023	-0.031	-0.026
40	1.606	1.625	0.019	-0.026	-0.03
45	1.605	1.63	0.025	-0.001	0.005
50	1.592	1.613	0.021	-0.013	-0.017

Appendix 2



Fig.14 Physical map of data collector

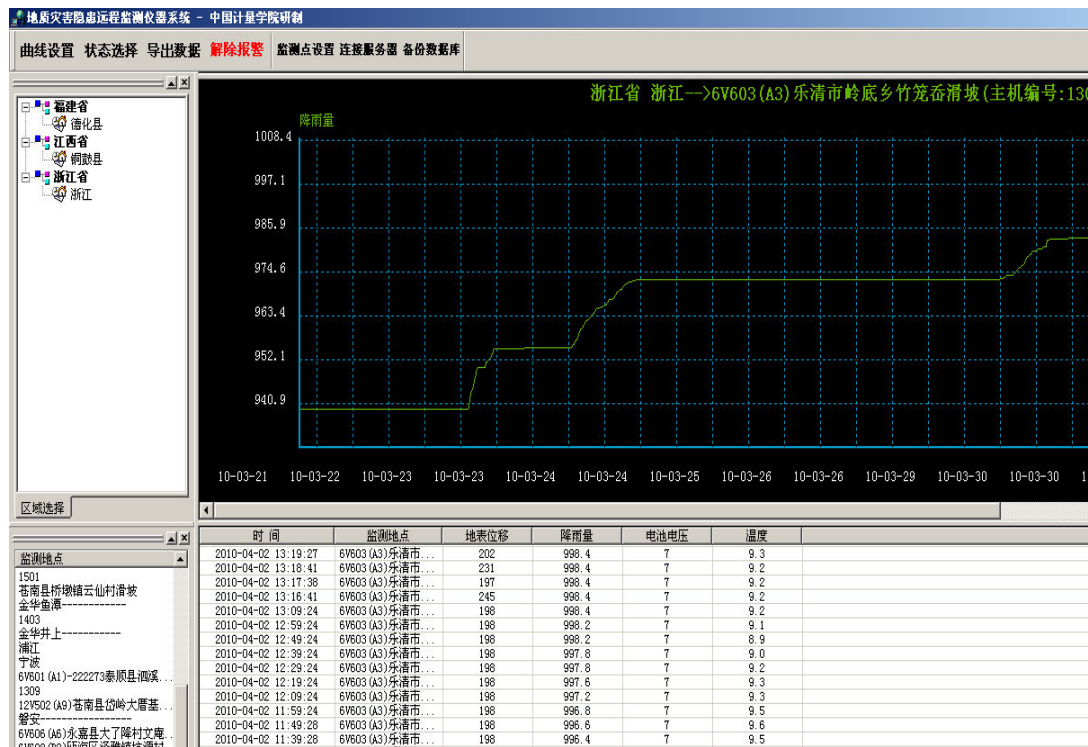


Fig.15 PC interface diagram